

An investigation of GNSS atomic clock behavior at short time intervals

Erin Griggs · E. Robert Kursinski ·
Dennis Akos

Received: 13 June 2013 / Accepted: 27 September 2013 / Published online: 15 October 2013
© Springer-Verlag Berlin Heidelberg 2013

Abstract A technique for obtaining clock measurements from individual GNSS satellites at short time intervals is presented. The methodology developed in this study allows for accurate satellite clock stability analysis without an ultra-stable clock at the ground receiver. Variations in the carrier phase caused by the satellite clock are isolated using a combination of common GNSS carrier-phase processing techniques. Furthermore, the white phase variations caused by the thermal noise of the collection and processing equipment are statistically modeled and removed, allowing for analysis of clock performance at subsecond intervals. Allan deviation analyses of signals collected from GPS and GLONASS satellites reveal distinct intervals of clock noise for timescales less than 100 s. The clock data collected from GPS Block IIA, IIR, IIR-M, and GLONASS satellites reveal similar stability performance at time periods greater than 20 s. The GLONASS clock stability in the 0.6–10 s range, however, is significantly worse than GPS. Applications that rely on ultra-stable clock behavior from the GLONASS satellites at these timescales may therefore require high-rate corrections to estimate and remove oscillator-based errors in the carrier phase.

Keywords Allan deviation · Clock analysis · GPS · GLONASS · Radio occultation

Introduction

The stability of GNSS satellite clocks is critical to precise timing and positioning applications. Corrections to the carrier phase from satellite clock instabilities can be necessary, as these variations limit the ability to distinguish delays from other sources. Radio occultation (RO) is a remote sensing technique that measures the delay in propagation of signals from the GPS satellites to infer physical characteristics about the atmosphere (Kursinski et al. 2000). GNSS RO has become one of the most important data sets for numerical weather prediction (Cardinali 2009). The addition of GLONASS is of particular interest for future occultation missions; more GNSS RO signal sources provide more frequent and denser sampling of the atmosphere, which improves weather forecasts (Harnisch et al. 2013). The GLONASS signals are frequency division multiple access and broadcast on different frequencies than GPS L1. Tracking the code division multiple access signals of GPS often results in lower signal-to-noise ratio (SNR) due to the overlapping spectra from each GPS satellite in view of the antenna (Bonnedal et al. 2012). GLONASS signals offer the potential of higher SNR, as their frequency bands are isolated from one another and from GPS L1.

Satellite clock instabilities cause variations in the carrier phase that will degrade the atmospheric profiling via RO if not properly characterized. A clock sampling interval of 1 s or less is required for single and undifferenced processing to achieve the highest quality excess atmospheric phase data for RO applications (Schreiner et al. 2009). Because a typical radio occultation event lasts approximately 100 s, knowledge of clock stability overtime intervals of 0.1–100 s is significant (Melbourne 2005). It is important to understand the behavior of GNSS satellite clocks as it influences

E. Griggs (✉) · D. Akos
University of Colorado, Boulder, CO 80309, USA
e-mail: erin.griggs@colorado.edu

E. R. Kursinski
Moog Advanced Missions and Science, Golden, CO 80401, USA

future RO receiver and satellite designs, as well as required ground infrastructure and postprocessing methodologies.

A common method used to characterize clock performance is the Allan deviation. Daly and Kitching (1990) characterized GPS and GLONASS clocks by performing an Allan deviation analysis using the time adjustment parameter given by the broadcast ephemerides. The clock parameter in the broadcast message is reported once every two hours, an interval too infrequent for short-term clock stability information needed for RO. Other publications have used carrier-phase-based interpolation and detrending methods to obtain Allan deviations for averaging intervals less than 30 s, but all utilized clock correction data from reference stations with ultra-stable atomic clocks (Hesselbarth and Wanninger 2008; Delporte et al. 2010; Gonzales and Waller 2007). Hauschild et al. (2012) present an in depth analysis of the Allan deviation for nearly every GNSS satellite, but concerns exist about their Kalman-filtered results. For instance, their Kalman-filtered clock estimation is significantly higher at $\tau \geq 10$ s than the one-way and three-way carrier-phase methods for the Block IIF satellite, PRN 25 (Hauschild et al. 2012). In addition, the thermal noise of the collection and processing equipment becomes a relevant source of error for time intervals less than and equal to 1 s and is not accounted for by these references.

Prior literature utilizes a global network of reference stations and/or highly stable atomic clocks to characterize on-board satellite clocks. In the present study, the raw carrier-phase measurements from a software receiver have been utilized to determine relative clock behavior between pairs of GNSS satellite clocks. When three satellites are tracked simultaneously, individual satellite clock behavior can be isolated via the triangulation method (Gray and Allan 1974). This approach works well as long as the instabilities of the three clocks are similar in magnitude. As will be described in detail below, the combination of single differencing and triangulation method removes the need for a very stable atomic oscillator at the receiver. It also allows for on-board GNSS oscillator characterization that is accessible to more potential users. The use of a software receiver, although not mandatory for clock isolation, allows for high-rate sampling and variation of the phase lock loop (PLL) bandwidth which, in turn, affect the SNR. The effect of the thermal noise can be isolated, modeled as white phase modulation, and removed statistically. What remains is the Allan deviation of the satellite clock of interest for intervals as short as 0.4 s.

An introduction to the Allan deviation and triangulation method developed by Gray and Allan (1974) is presented in the next section. A description of additional processing techniques used in this study is given in the following section. As both the GPS and GLONASS constellations are

important signal sources for RO missions, an analysis of the Allan deviation derived from their clock phases is presented for averaging intervals between 0.4 and 100 s. The source of the clock noise is hypothesized for different averaging intervals. Finally, the clock instabilities are translated to maximum error in carrier phase, and the time interval at which the clock must be corrected to reduce the residual error below a desired threshold is discussed.

Allan deviation

The Allan deviation or its square, the Allan variance, is a common statistic used to characterize the performance of oscillators. Also known as the two-sample variance, the Allan variance describes the clock behavior as a function of the time period between samples, τ . The resultant behavior often follows certain slope characteristics based upon the type of noise measured.

The average fractional frequency of the i^{th} clock phase measurement over the interval τ is given by

$$\bar{y}_i^\tau = \frac{x(t_i + \tau) - x(t_i)}{\tau} \quad (1)$$

where $x(t)$ is the time deviation of a signal. The Allan variance is defined as the infinite average of the difference between subsequent fractional frequency measurements and is given by

$$\sigma_y^2(\tau) = \frac{1}{2} E(\Delta \bar{y}^\tau)^2 \approx \frac{1}{2(M-1)} \sum_{i=2}^{M-1} (\bar{y}_{i+1}^\tau - \bar{y}_i^\tau)^2 \quad (2)$$

where $\Delta \bar{y}^\tau$ is the difference in adjacent fractional frequency measurements, and $M = N - 1$ is the number of frequency samples, and N the number of time samples. Equation (2) makes use of an overlapping estimate of the expected value of the fractional frequency measurements (Allan et al. 1988).

The variance of a single oscillator can be estimated by comparison with data from two or more other oscillators. The triangulation method requires independent oscillators and offers an unbiased result because the expected value of the cross-correlation term approaches zero as the number of measurements increases (Gray and Allan 1974). This study utilizes a version of the triangulation methodology that isolates individual satellite clocks and resolves the receiver clock noise by substituting single-differenced carrier-phase measurements. Differencing carrier-phase measurements from two satellites is a common method used to remove the errors caused by the receiver clock. The remainder is the difference in clock phase between a pair of satellites with essentially no noise contribution from the receiver clock.

If the difference of consecutive average fractional frequency measurements from a particular clock A is defined as

$$\epsilon_A(t_i) = \frac{1}{\tau}(x_A(t_i + \tau) - 2x_A(t_i) + x_A(t_i - \tau)) \tag{3}$$

then the application of the triangulation method using single difference pairs with clocks B and C is given by

$$\begin{aligned} & \frac{1}{2} \frac{1}{(N-2)\tau^2} \sum_{i=2}^{N-2} (\epsilon_A(t_i) - \epsilon_B(t_i)) * (\epsilon_A(t_i) - \epsilon_C(t_i)) \\ &= \frac{1}{2(N-2)\tau^2} \left(\begin{aligned} & \sum_{i=2}^{N-2} \epsilon_A^2(t_i) - \sum_{i=2}^{N-2} \epsilon_A(t_i)\epsilon_C(t_i) \\ & - \sum_{i=2}^{N-2} \epsilon_B(t_i)\epsilon_A(t_i) + \sum_{i=2}^{N-2} \epsilon_C(t_i)\epsilon_B(t_i) \end{aligned} \right) \\ & \cong \frac{1}{2(N-2)\tau^2} \sum_{i=2}^{N-2} \epsilon_A^2(t_i) = \sigma_{y,A}^2 \end{aligned} \tag{4}$$

As the cross-correlation terms between different satellite clocks approach zero with increasing number of observations, the squared error term from the satellite of interest remains. This is approximately equivalent to the Allan variance of the clock phase error from satellite A , to within the error of the accumulated cross-correlation terms.

The number of measurements N that is sufficient for the cross-multiplied satellite terms to be significantly less than the squared term can be estimated as follows. The standard deviation of a single element in the cross-term summation of (4) is

$$\langle (\epsilon_A \epsilon_B)^2 \rangle^{1/2} = \langle (\epsilon_A^2 \epsilon_B^2) \rangle^{1/2} = \langle \epsilon_A^2 \rangle^{1/2} \langle \epsilon_B^2 \rangle^{1/2} = \sigma_{y,A} \sigma_{y,B} \tag{5}$$

The second equality is valid because the values ϵ_A and ϵ_B from the clocks of two different satellites A and B are assumed independent and zero mean. The standard deviation of each of the three cross-term summations will approximately equal $\sigma_{y,A}\sigma_{y,B}/N$. If the desired fractional uncertainty in the estimate of $\sigma_{y,A}^2$ is denoted as m , then

$$\frac{\sigma_{y,A}\sigma_{y,B} + \sigma_{y,A}\sigma_{y,C} + \sigma_{y,C}\sigma_{y,B}}{N} = m\sigma_{y,A}^2 \tag{6}$$

If the three frequency standards have comparable stability, such that $\sigma_{y,A} \sim \sigma_{y,B} \sim \sigma_{y,C}$, then $N = 3/m$. If an uncertainty of 10 % ($m = 0.1$) in the $\sigma_{y,A}^2$ estimate is desired, then $N = 30$; at least thirty measurements of the carrier phase from each satellite would be necessary to determine the variance of a single satellite clock. If one of the three frequency standards was a factor of 10 worse than the other two, such that $\sigma_{y,A} \sim \sigma_{y,B} \sim 0.1\sigma_{y,C}$, then $N = 21/m$. To

achieve 10 % uncertainty in the $\sigma_{y,A}^2$ estimate, 210 measurements would be required.

This triangulation methodology does not require an atomic reference for the receiver. In fact, the receiver clock needs only enough precision to maintain a tight phase lock on all signals, as single differencing removes the error introduced by the common receiver clock. Multiplying pairs of single differences allows for Allan deviation analysis of a single satellite clock, and in turn, its stability characteristics can be determined given comparable clock stabilities and enough measurements. In this study, the overall data arc length, data volume considerations, and the variation in orbit and atmospheric errors limit the applicability of this methodology to time intervals of approximately 1,000 s.

Data collection of GNSS satellites

On June 25, 2012, raw GPS data were collected from a rooftop antenna at the University of Colorado in Boulder. A Trimble Zephyr Geodetic antenna capable of collecting GPS L1, L2, and L5, as well as GLONASS L1, L2, and L3, was used. A GPS SiGe module, a raw intermediate frequency (IF) sample collector developed by the University of Colorado, was used (Borre et al. 2007). The raw signal was sampled at a rate of 4 Msps, and approximately 1,000 s of data were collected. The GPS clock types and satellite blocks sampled in this experiment are shown in Table 1.

Raw GLONASS data were collected on July 27, 2012, from the same location. The same antenna was utilized, but a Universal Software Radio Peripheral (USRP) front-end was used to collect and sample the raw signal because the GLONASS nominal frequency is outside the capability of the SiGe module. The raw signal was sampled at a rate of 10 Msps, and a longer data set of approximately 1,500 s was collected. The clock types, frequency channels, and almanac numbers are shown in Table 2.

Processing the raw IF samples with a software receiver provides the greatest possible flexibility in the receiver

Table 1 GPS satellite clock data collected

PRN	SVN	Block	Launch date	Clock type
7	48	IIR-M	03/15/2008	Rb3
8	38	IIA	11/06/1997	Cs4
13	43	IIR	07/23/1997	Rb1
23	60	IIR	06/23/2004	Rb2
19	59	IIR	03/20/2004	Rb3
3	33	IIA	03/28/1996	Cs4

Shown are the PRN number of the satellite, satellite vehicle number (SVN), satellite block, satellite launch date, and atomic clock type (National Geospatial-Intelligence Agency, referenced in 2012; United States Naval Observatory, referenced in 2012)

Table 2 GLONASS satellite data collected

Almanac	SVN	Frequency channel	Launch date	Clock type
11	723	0	12/25/2007	Cs
21	725	4	09/25/2007	Cs
10	717	−7	12/25/2006	Cs
22	731	−3	03/02/2010	Cs
20	719	2	10/26/2007	Cs
21	701	−5	02/26/2011	Cs

Shown are the orbital slot/almanac number, SVN, frequency channel, satellite launch date, and atomic clock type. Note that SVN 701 is also assigned orbital slot number 21, but was marked as in “Flight Tests” and was not used for this study (Information-Analytical Center, referenced in September 2012)

configuration for satellite clock analyses. Many commercial off-the-shelf (COTS) receivers have limited flexibility in the choice of loop bandwidth and measurement rate, both of which are easily adjustable in the software receiver. The variable bandwidths of a software receiver allow for the detection of white phase modulation at short time-scales, where it dominates the Allan deviation.

The satellite clocks analyzed in this study are rubidium and cesium atomic frequency standards on-board present GNSS satellites. The methodology developed here can be applied to other GNSS constellations, such as the passive hydrogen masers on the Galileo satellites and the frequency references on the Compass/Beidou satellites. The timing system of the GPS Block IIA satellites consists of two cesium atomic frequency standards and two rubidium atomic frequency standards, while the IIR and IIR-M blocks carry only rubidium standards. The current generation of GLONASS satellites, GLONASS-M, relies solely on cesium standards (Hauschild et al. 2012). As all atomic clocks are passive frequency standards, a voltage-controlled crystal oscillator (VCXO) is frequency locked to the free-running atomic standard via a control loop. The phase, frequency, and frequency drift of the time keeping system (TKS) output on the GPS satellites are fine-tuned from ground control and adjusted to cancel drifts in the atomic frequency output or anomalous frequency departures. A comparison is made between the frequencies of the VCXO and the atomic reference, and the relative difference is used to adjust the frequency of the VCXO (Petzinger et al. 2002). It has been noted that the existing frequency meter is the primary cause of short-term timing instability in the Block IIR TKS for times less than 100 s (Dass et al. 2002).

Comparison to reference stations

For this study, delay variations induced on the signal phase due to propagation through the ionosphere and troposphere

were assumed to be constant for each satellite over the short observation intervals. The delays were not assumed equal between pairs of satellites, however. Multipath has been minimized through unobstructed rooftop placement of the antenna. Residual ionospheric, tropospheric, and multipath errors are assumed to be small and were removed with polynomial detrending (Delporte et al. 2010; Hauschild et al. 2012). Short-term ionospheric path delay variations due to scintillation could be interpreted as clock variations; therefore, to justify this simplification, the quality of the detrended clock measurements was compared against clock corrections produced by the International GNSS Service (IGS) and center for orbit determination in Europe (CODE).

When the receiver clock is less stable than the GNSS clock, the error generated by the receiver clock masks the underlying GNSS satellite clock behavior. Under these conditions, comparison of clock phase from a single satellite is not feasible. Single differenced pairs of satellites remove the receiver clock error and can be compared directly to the same single differenced pairs from IGS or CODE. The IGS produces a precise clock correction for the GPS satellites at a 30-s rate and CODE at a 5-s rate (Senior et al. 2008). Agreement between the data sets serves as a validity check on the clock phase obtained from the carrier-phase measurements from the software receiver.

Figure 1 shows the GPS clock offsets as produced by the IGS (30 s), CODE (5 s), and the software receiver (0.05 s) for the PRN 7/PRN 13 difference pair. Senior et al. (2008) states that the precision of the IGS clock products is approximately 1 cm (33 ps) and the accuracy about 3 cm (100 ps). The root-mean-square (RMS) differences shown in Table 3 are within these stated precision limits, thus validating our assumption that the variations in the differential ionospheric, tropospheric, and multipath delays were negligible during these collections.

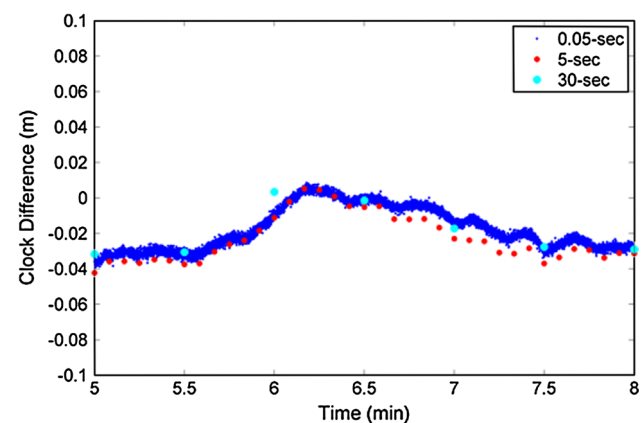


Fig. 1 Plot of 0.05 s (software receiver), 5 s (CODE), and 30 s (IGS) GPS clock differences for the PRN 7/PRN 13 pair for 3 min on June 25, 2012. The software receiver is able to show higher resolution fluctuations in the clock phase not present in the CODE and IGS data

Table 3 The RMS of the differences between this experiment and values for concurrent times reported by IGS and CODE, in picoseconds

Difference pair (PRN)	IGS (ps)	CODE (ps)
7/19	30	14
7/23	34	24
7/3	26	22
7/8	64	24
7/13	27	17

Single differencing with data from PRN 7 was performed for all data sets

Thermal noise reduction

The thermal noise of the receiver contributes to the variations in the measured clock phase and, in fact, dominates for sufficiently short time intervals. The Allan deviation of the satellite clock can be analyzed in greater detail at shorter time intervals if the thermal noise can be removed. If the PLL bandwidth is decreased, the carrier-phase observations become less noisy, and the Allan deviation decreases. However, as the bandwidth is reduced, there exists a bandwidth threshold below which the software receiver loses lock on tracking the signal. The inherent stability of the receiver clock and relative satellite dynamics is essential in determining the lower limit on the bandwidth; an atomic reference could allow tracking at a lower bandwidth. Heuristically, it was found that PLL bandwidths less than 20 Hz caused tracking issues for these particular data sets. A different method to overcome the signal processing noise is to increase the carrier-to-noise power density (C/N_0) of the signal. The strength of the GNSS signals could be increased by using an antenna with higher gain. However, higher gain antennas become increasingly directional, which limits the ability to capture signals from multiple satellites concurrently and eliminates the ability to use paired differencing to isolate individual satellite clocks.

Another method of decreasing the thermal noise is to average sequential clock phase values. This reduces the short-term phase variations by essentially narrowing the filter bandwidth. Because the C/N_0 varies by a few dB-Hz between the satellites collected in this study, averaging serves to eliminate excess noise where C/N_0 is relevant. The optimum performance is achieved when the noise bandwidth is the inverse of the sampling interval. For example, using 20 Hz data, 40 clock phase points were averaged to determine the $\tau = 2$ s Allan deviation values. This phase averaging serves to distinguish between white and frequency phase modulation noises, and behaves like a modified Allan deviation (Riley 2008).

At longer timescales, the Allan deviation of a GNSS atomic clock typically behaves as white frequency modulation whose characteristic slope on a log–log scale is $\tau^{-1/2}$. The expected slope of the averaged measurements, when dominated by the receiver thermal noise at shorter time intervals (which produces white phase noise), is $\tau^{-3/2}$, as seen in Fig. 2 for $\tau \leq 0.4$ s (Riley 2008). To isolate and remove the contribution of the white phase noise to the measured Allan deviations, the coefficients of the linear fit (in log–log space) were determined using the data points for the first four values of $\tau = 0.05, 0.1, 0.15$, and 0.2 s. The uncertainty of the Allan deviation estimates at these shorter time intervals is small because of their large number of phase estimates over the entire data acquisition period. Under the assumption that thermal noise and satellite clock noise are the only contributors to the measured variance at these timescales, the thermal noise can be removed statistically using the linear model to extrapolate the white phase noise contribution to longer time intervals, leaving only the satellite clock noise contribution. Figure 2 illustrates the removal of the thermal noise with a $\tau^{-3/2}$ model of the white phase noise. The smooth, straight line behavior shown for all satellites for $\tau \leq 0.4$ s is an artifact of the data collection and sampling hardware and is removed to reveal the underlying performance of the satellite clock.

To ensure that the clock noise estimate was really from the clock, only cases are reported where the residual between the total measured Allan deviation and the white phase noise fitted lines was at least three times larger than the RMS uncertainty in the white phase noise contribution. The dashed values shown in Fig. 2 are the Allan deviations with thermal noise variance removed. Note that, not all GPS satellites have values $\tau = 0.4$ and 0.5 s because of the 3σ quality check.

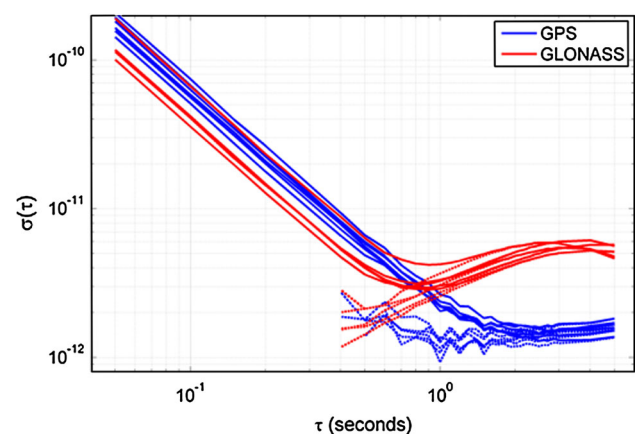


Fig. 2 GNSS short-term Allan deviations before and after thermal noise removal. The dashed values are the Allan deviations after subtraction of the linear model of the white phase noise

Adjustments Associated with the Limited Number of Samples

The triangulation technique of Gray and Allan (1974) modified with single differenced clock phase data that we use here can yield underestimates of the Allan variance when the number of samples is limited. Such a negative bias in the estimate occurs when the number of samples is insufficient to make the cross-correlation terms in (3) be negligible. Under these conditions, the Allan variance estimate can be abnormally low or even negative.

We have simulated this effect and developed a simple approach to mitigate it. When negative values appear in the summation operator in (3), two different summations are performed. In the first summation, the negative values in the summation operator in (3) are set to zero, such that the summation in (3) produces an underestimate of the Allan variance. In the second summation, only the positive values are summed, which reduces the number of terms in the summation and yields an overestimate of the Allan variance. These two estimates are then averaged, producing an estimate closer to the true Allan variance. This approach was found to significantly improve the Allan variance estimates based on simulations.

The Allan deviation values can vary significantly over short time intervals, especially for larger values of τ where fewer data points exist for the averaging intervals. To reduce the spread, the measurements were smoothed using a spline interpolator of order three to better reveal the general behavior represented by the noisy estimates of the Allan deviation.

Allan deviation analysis

Plots of the Allan deviation are presented for all satellites present in the data sets obtained by our GNSS data acquisition system. As noted above, the clock phase values were averaged to reduce signal processing noise, and cubic spline interpolation was used to smooth over noisy results due to the limited length of our data set. The additional phase averaging allows for differentiation between white and flicker phase modulation and behaves similarly to a modified Allan deviation. The thermal noise was characterized as white phase noise and removed statistically.

Results for the Allan analysis of the six GPS satellite data sets collected are shown in Fig. 3. Between $\tau = 1$ and 20 s, the Allan deviation values exhibit a positive slope. This differs distinctly from the white frequency noise of passive atomic standards at longer timescales. The positive slope for these time periods is presumably the result of frequency locking a crystal oscillator to a passive atomic standard. Although not entirely obvious from the

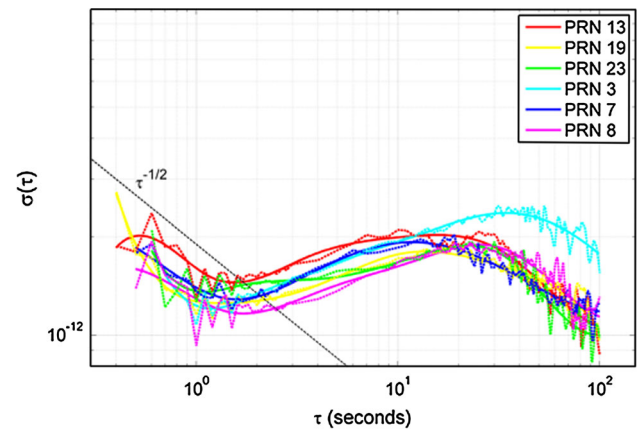


Fig. 3 Individual GPS satellite Allan deviation for PRNs 13, 19, 23, 3, 7, and 8. The *dashed* raw values are smoothed by cubic spline interpolation. The slope of $\tau^{-1/2}$ is shown for reference

timescales shown, the slope of the Allan deviation closely approaches $\tau^{-1/2}$ for averaging intervals larger than 30 s. This is expected for white frequency noise that results from frequency locking in passive standards (International Radio Consultative Committee 1986). This is typical longer-term behavior of cesium and rubidium frequency standards. The upturn in the Allan deviation at timescales shorter than 1 s suggests white frequency noise modulation for a modified Allan deviation (Riley 2008).

Despite the different GPS satellite blocks being compared here, the Allan deviation values are similar for all averaging intervals. PRNs 3 and 8 are both Block IIA satellites and utilize cesium oscillators, while the remaining satellites are Block IIR and IIR-M satellites and use rubidium standards. At longer timescales, PRN 3 exhibits the worst Allan deviation, likely due to a combination of degraded performance with age and improved clock technology over the 17 years since its launch.

Allan deviation results for the five measured GLONASS satellites are shown in Fig. 4. A positive slope for the Allan deviation occurs for values of τ less than and including $\tau = 3.5$ s. This noise is not characteristic of the atomic portion of cesium standards and is likely due to a combination of the crystal oscillator frequency locked to the cesium standard and the response of the frequency locked control loop. For timescales larger than approximately $\tau = 10$ s, the Allan deviation decreases at approximately $\tau^{-1/2}$, corresponding to white frequency noise (International Radio Consultative Committee 1986).

Figure 5 compares the GLONASS and GPS Allan deviation results, including the maximum 3σ error envelope based upon the raw estimates. The Allan deviation estimates for both constellations overlap for larger values of τ , where the white frequency noise corresponding to atomic clock stability is the primary source of phase error.

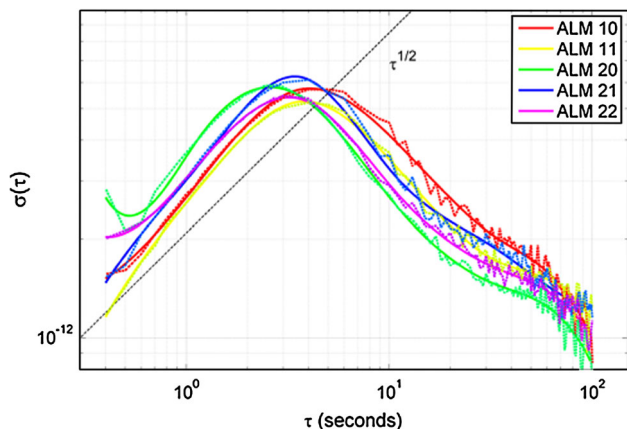


Fig. 4 Individual GLONASS satellite Allan deviation for ALMs 10, 11, 20, 21, and 22. The *dashed* raw values are smoothed by cubic spline interpolation. The slope of $\tau^{1/2}$ is shown for reference

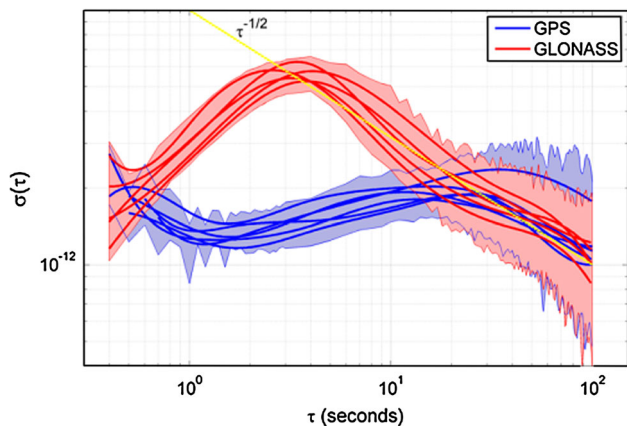


Fig. 5 Comparison of the smoothed GPS and GLONASS Allan deviation values. Color coordinated 3σ error bar envelopes calculated from the raw measurements are shown for each constellation. The characteristic slope for white frequency noise is shown for comparison

The $\tau^{-1/2}$ slope is also shown for reference at longer timescales. The fundamental difference between the two GNSS constellations is apparent in the interval of $0.6 \leq \tau \leq 20$ s, where the clock stability of the GLONASS satellites is notably worse than GPS.

Estimates from this study can be compared to other published results with Allan deviation estimates corresponding to values of τ that overlap with the short-term results found here. At $\tau = 100$ s, it is assumed that the clock noise is behaving as white frequency modulation. Thus, a rough comparison can be made to other studies at this interval, noting that the results from this analysis are similar to a modified Allan deviation, and should behave as approximately $1/\sqrt{2}$ of the traditional Allan deviation (Riley 2008). Table 4 displays the Allan deviation values, all normalized by 10^{-12} , at $\tau = 100$ s for two other studies for comparison.

Table 4 Comparison of bandwidth averaged Allan deviation values as reported by this study, the traditional Allan deviations in Hauschild et al. (2012), and modified Allan deviations in Senior et al. (2008) at $\tau = 100$ s. Values are round to the nearest 10^{-13} value. PRN 7 is not reported in the latter study because SVN 37 was replaced by SVN 48 in 2008

GPS Satellite	Hauschild et al. (2012)	Senior et al. (2008)	Griggs et al. (2013)
PRN 3	2.0	1.6	1.8
PRN 7	1.6	–	1.2
PRN 8	2.2	1.6	1.1
PRN 13	1.7	1.1	1.1
PRN 19	1.5	1.1	1.1
PRN 23	1.4	1.1	1.0

The largest discrepancy appears to be with the Block IIA satellites, where our study yields a lower estimate of the 100 s Allan deviation for PRN 8 and a higher estimate for PRN 3. The Allan deviations for the Block IIR and IIR-M are within 10 % of the results from the other studies at this time interval.

At $\tau = 1$ s, the Allan deviation results cannot be directly compared with studies that use a traditional Allan deviation, as difference between white and flicker phase modulation is not discernible. It is noted, however, that Hesselbarth and Wanninger (2008) show similar characteristics in their GLONASS Allan deviation results between $\tau = 1$ and 10 s to what is shown in this study. In contrast to other studies, the noise generated from the receiver’s internal processing was reduced in the present study, allowing for the true satellite clock stability at $\tau = 1$ s to be exposed.

Additional applications/implications

Carrier-phase errors caused by satellite clock instability can be reduced with periodic corrections. For example, clock corrections given by the IGS allow for the GPS clock error to be corrected every 30 s. The maximum residual error between applied clock corrections can be estimated using linear interpolation of the clock phase measurements. The following set of equations relates the residual error to the Allan deviation.

The linearly interpolated estimate of a clock phase at the midpoint between two phase measurements separated in time by 2τ is given as follows,

$$\hat{\phi}(t) = \frac{\phi(t + \tau) + \phi(t - \tau)}{2} \tag{7}$$

The error in this estimate is the difference between the estimate and the true clock phase at time,

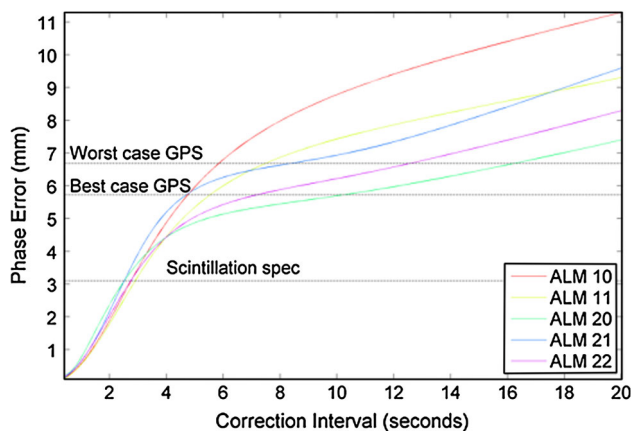


Fig. 6 Necessary clock corrections for phase error thresholds for collected GLONASS satellite clocks. The phase error for the worst- and best-case GPS results from this study with 30-s IGS clock corrections applied is shown for reference. The scintillation phase error specification is set to 0.1 radians/10 s, resulting in a phase error of about 3.1 mm

$$\varepsilon_{\phi(t)} = \hat{\phi}(t) - \phi(t) = \frac{\phi(t + \tau) - \phi(t)}{2} + \frac{\phi(t) - \phi(t - \tau)}{2} \quad (8)$$

The error in the estimated interpolated clock phase is similar in form to the definition of Allan variance, described in (2). The expected error in the estimate can therefore be related to the Allan variance as follows,

$$\langle \varepsilon_{\phi(\tau)}^2 \rangle = \frac{\sigma^2(\tau)\tau^2}{2} f^2 \quad (9)$$

where f is the frequency of the signal, and the clock phase error is in units of cycles.

An Allan deviation at a certain time interval can be used to determine the maximum error in clock phase. From this, the rate of clock corrections required to obtain a desired error threshold can be determined. Figure 6 presents a plot of the rate of corrections required for the various GLONASS clocks to maintain a particular phase error. The dotted horizontal lines represent phase error requirements corresponding to the best- and worst-case results from the GPS satellites collected in this study with 30-s IGS clock corrections applied. From these, the time interval necessary between corrections of the GLONASS clocks can be determined. In general, more frequent corrections of the GLONASS satellite clocks are necessary to achieve the same phase error levels as GPS. Corrections at 6-s intervals would be needed if the phase errors from all GLONASS clocks were required to match those of the worst-case GPS satellite collected in this study. To match the best-case GPS satellite from this study, 4-s clock corrections would be needed for the GLONASS satellites. The lowest horizontal line is a measurement requirement of 0.1 radians over 10 s in order to measure phase variations due to ionospheric scintillations (P. Straus, pers. comm.). To achieve this level

of accuracy, GLONASS clock corrections would be needed approximately every 2 s.

Summary and conclusions

We have presented an approach for isolating the stability of individual GNSS satellite clocks. Single differencing of carrier-phase measurements from pairs of satellites removed the need for an atomic reference at the receiver. To analyze the Allan deviation of a single satellite clock, pairs of single differences were multiplied and summed, which reduced the influence of noise from the other satellites and isolated the behavior of the clock of interest. The white phase noise contribution from the receiver and processing equipment was modeled and eliminated to better isolate the clock performance at shorter timescales. The methodology developed in this study is straight forward to implement, does not require tracking stations with ultra-stable receiver clocks, and allows assessment of satellite clocks from any GNSS constellation at short timescales.

The stability of a subset of the GPS and GLONASS satellite clocks was measured and compared for time intervals ranging from 0.4 s to 100 s. The constellations exhibited similar behavior for averaging intervals >20 s. The smooth slope of the Allan deviations corresponded to white frequency noise, typical behavior of passive atomic standards for this time interval. The Allan deviation of the GLONASS clocks from 0.6 to 10 s was significantly worse than the GPS results, with the largest difference occurring between $\tau = 2$ and 4 s. The larger Allan deviations across these time intervals are likely due to a combination of the crystal oscillators locked to the cesium standards and the performance of the frequency locking control loop in the GLONASS cesium frequency standards.

Additional averaging of the data would be necessary if stabilities of the clocks in the trio of satellites were grossly different. For example, if one of the three frequency standards was a factor of ten better than the other two, as with the Block IIF rubidium clocks compared to the older GPS, then to achieve 10 % uncertainty in the σ_A^2 estimate would require 1,200 averages. The Allan deviation at a timescale of 100 s would require 120,000 s, or almost 1.5 days, of data collection. A better option is to simultaneously acquire data from three GNSS satellites with clocks of comparable stability. To estimate Block IIF rubidium, performance would require some combination of three Block IIF satellites on rubidium standards and Galileo satellites in the sky at the same time.

We plan to collect longer data sets with a larger variety of GNSS satellite clocks at the National Institute of Standards and Technology in Boulder, CO. By using an ultra-

stable clock at the receiver, the GNSS clock stability will be estimated both directly against the ultra-stable clock and via the combined single differencing triangulation method presented here. We will evaluate the combined single differencing and triangulation technique against the direct estimates. Acquisition of a longer data set will provide higher certainty in the Allan deviation estimates at longer time intervals, although dual frequency acquisition may be necessary for longer collections. We intend to perform a similar analysis to characterize Galileo, Compass/BeiDou, and GPS Block IIF satellite clocks. Some of the clocks from newer constellations, such as GPS Block IIF and Galileo, will have Allan deviations considerably better than the clocks analyzed in this study.

For applications utilizing GLONASS satellites for high-rate carrier-phase data, users may assess their oscillator stability needs against our findings here. GLONASS clock instability appears to peak between 2 and 6 s and therefore would require clock corrections to estimate and remove oscillator-based errors if stability comparable to GPS is required. To remove the GLONASS short-term clock errors, higher rate clock products are necessary. This may be provided by high-rate ground or space-based receivers, or by the IGS or another analysis center capable of providing clock solutions.

Acknowledgments The authors would like to thank the reviewers, particularly Jim Ray, for their thorough assessment and appreciate their comments and suggestions, which significantly contributed to improving the quality of the publication. We acknowledge Moog Advanced Missions and Science for sponsorship of this study. The data sets used in this study were obtained using equipment supplied by the University of Colorado at Boulder. Precise ephemerides and reference clock products were provided by the International GNSS Service and the Center for Orbit Determination in Europe.

References

- Allan D, Hellwig H, Kartaschoff P, Vanier J, Vig J, Winkler G, Yannoni N (1988) Standard Terminology for Fundamental Frequency and Time Metrology, Proc. 42nd Annu. Freq. Control Symp., pp.419-425 1988 :IEEE Press
- Bonnedal M, Christensen J, Carlström A, Lindgren T, Marquardt C, von Engeln A, Andres Y, Larsen G, Lauritsen K, Syndergaard S, Benzon H, Sørensen M, Gorbunov M, Kirchengast G, Pirscher B, Schweitzer S, Fritzer J, Montenbruck O, Zus F, Beyerle G (2012) GRAS Radio Occultation Performance Study, Issue 3 Draft, RUAG Space AB, Göteborg, Sweden, pp.73-4,182-3,P-GRDS-REP-00002-RSE
- Borre K, Akos D, Bertelsen N, Rinder P, Jensen S (2007) A Software-Defined GPS and Galileo Receiver: A Single-frequency Approach. Birkhäuser, Boston
- Cardinali, C (2009) Forecast sensitivity to observation (FSO) as a diagnostic tool, ECMWF Technical Memorandum., pp 599:626
- Daly P, Kitching I (1990) Characterization of NAVSTAR GPS and GLONASS On-Board Clocks. IEEE AES Mag., July, pp. 3–9, 0885/8985/90/0700/0003
- Dass T, Freed G, Petzinger J, Rajan J (2002) GPS Clocks in Space: Current Performance and Plans for the Future, Proc. 34th Annu. Precise Time and Time Interval Meet., pp. 175–192
- Delporte J, Boulanger C, Mercier F (2010) Simple Methods for the Estimation of the Short-term Stability of GNSS On-board Clocks, Proc. 42nd Annu. Precise Time and Time Interval Meet., pp.215–224
- Gonzales F, Waller P (2007) Short term GNSS clock characterization using One-Way carrier phase, IEEE, pp. 517–522, 1-4244-0647-1/07/
- Gray J, Allan D (1974) A Method of Estimating the Frequency Stability of an Individual Oscillator. Proc. 28th Annu. Freq. Cont. Symp., pp.243–246
- Harnisch F, Healy S, Bauer P, English S (2013) Scaling of GNSS radio occultation impact with observation number using an ensemble of data assimilations, ECMWF Technical Memorandum., pp. 693:26
- Hauschild A, Montenbruck O, Steigenberger P (2012) Short-term analysis of GNSS clocks. GPS Solut. 17(3):295–307. doi:10.1007/s10291-012-0278-4
- Hesselbarth A, Wanninger L (2008) Short-term Stability of GNSS Satellite Clocks and its Effects on Precise Point Positioning, Proc. ION GNSS-2008, Institute of Navigation, pp. 1855–1863
- Information-Analytical Center (IAC) (2012) GLONASS Constellation Status, 09.12.2012, www.glonass-center.ru/en/GLONASS/
- International GNSS Service (IGS) (2012) IGS Products, [ftp://cddis.gsfc.nasa.gov/](http://cddis.gsfc.nasa.gov/)
- International Radio Consultative Committee (1986) Characterization of frequency and phase noise. Rep. 580–2:142–150
- Kursinski E, Hajj G, Leroy S, Herman B (2000) The GPS Radio Occultation Technique, *TAO*, V11(1):53–114, March
- Melbourne W (2005) Radio Occultation Using Earth Satellites. Wiley-Interscience, Hoboken
- National Geospatial-Intelligence Agency (NGA) (2012) Current GPS Satellite Data. <http://earth-info.nga.mil/GandG/sathtml/satinfo.html>
- Petzinger J, Reith R, Dass T (2002) Enhancements to the GPS Block IIR Timekeeping System, Proc. 34th Annu. Precise Time and Time Interval Planning Meet., pp. 89–107
- Riley, W (2008) Handbook of Frequency Stability Analysis, Natl. Inst. Stand. Technol. Spec. Publ., US Dept. of Commerce, Boulder, CO, pp.9–11
- Schreiner W, Rocken C, Sokolovskiy S, Hunt D (2009) Quality assessment of COSMIC/FORMOSAT-3 GPS radio occultation data derived from single- and double-difference atmospheric excess phase processing. GPS Solut. 14(1):13–22
- Senior K, Beard R, Ray J (2008) Characterization of periodic variations in the GPS satellite clocks. GPS Solut. 12(3):211–225
- United States Naval Observatory (USNO) (2012) GPS Constellation Status. [ftp://tycho.usno.navy.mil/pub/gps/gpstd.txt](http://tycho.usno.navy.mil/pub/gps/gpstd.txt)

Author Biographies



Erin Griggs is a graduate student in Aerospace Engineering Sciences at the University of Colorado at Boulder. She received her B.S. and M.S. in Mathematical and Computer Sciences from Colorado School of Mines. Her research interests include GNSS signal processing algorithms, atomic clock analysis, orbital mechanics, and radio occultation receiver design.



Dennis Akos completed his Ph.D. degree in Electrical Engineering at Ohio University and is currently an Associate Professor in Aerospace Engineering Sciences at the University of Colorado at Boulder with visiting appointments at Luleå Technical University and Stanford University. His research interests include GNSS systems, software defined radio, applied/digital signal processing, and radio frequency design.



E. Robert Kursinski completed his Ph.D. degree in Planetary Sciences from the California Institute of Technology and is the Chief Scientist at Moog Advanced Missions and Science. His research focus is atmospheric remote sensing, particularly tied to the hydrological cycle and climate change.